Available online at www.sciencedirect.com

ScienceDirect

IFAC PapersOnline CONFERENCE PAPER ARCHIVE

IFAC PapersOnLine 54-20 (2021) 406–411

Input-output Data-driven Modeling and MIMO Predictive Control of an RCCI Engine Combustion

Behrouz Khoshbakht Irdmousa [*] , **Jeffrey Donald Naber** [*]
Javad Mohammadpour Velni [**] , **Hoseinali Borhan** [***] , **Mahdi Shahbakhti** [****]

[*] *Michigan Technological University, Houghton, MI 49931, USA (e-mails: bkhoshi, jnaber@mtu.edu)*
[**] *University of Georgia, Athens, GA 30602, USA (e-mail: javadm@uga.edu)*
[***] *Cummins Inc, Columbus, IN 47201, USA (e-mail: hoseinali.borhan @cummins.com)*
[****] *University of Alberta, Edmonton, AB, Canada T6G 1H9 (e-mail: mahdi @ualberta.ca)*

Abstract: This study presents a data-driven identification method based on Kernelized Canonical Correlation Analysis (KCCA) approach to generate a state-space Linear Parameter-Varying (LPV) dynamic representation for the RCCI engine combustion. An LPV model is used to estimate RCCI combustion phasing (CA50) and indicated mean effective pressure (IMEP) based on fuel injection timing and quantity. The proposed data-driven method does not require prior knowledge of the plant model states and adjusts number of states to increase the accuracy of the identified state-space model. The results demonstrate that the proposed data-driven KCCA-LPV approach provides a dependable technique to establish a fast and reasonably accurate RCCI combustion model. The established model is then incorporated in a design of a constrained MIMO Model Predictive Controller (MPC) to track desired crank angle for 50% fuel burnt and IMEP at various engine conditions. The controller performance results demonstrate that the established data-driven constrained MPC combustion controller can follow desired CA50 and IMEP with less than 1.5 CAD and 37 kPa error, respectively.

1. INTRODUCTION

Low Temperature Combustion (LTC) strategies are among promising candidates to help in meeting future emission and fuel economy requirements for Internal Combustion Engines (ICEs). LTC strategies are developed into various forms and Reactivity Controlled Compression Ignition Combustion (RCCI) is one of the most recently developed LTC strategies. Researchers have been studying to develop an RCCI combustion controller since the introduction of the RCCI strategy. These studies can be classified into simulation studies and experimental studies according to controller verification platform. Simulation studies implemented a validated RCCI engine models to test the controller performance. On the other hand, experimental studies tested the established RCCI combustion controller on an actual RCCI engine. Model-based simulation control study on RCCI combustion was initiated by Sadabadi et al. (Khodadadi Sadabadi et al., 2016). They developed a Linear Quadratic Regulator (LQR) based on their control-oriented RCCI engine model. Indrajauna et al. (Indrajuana et al., 2016) created a control-oriented model by linearizing a multi-zone RCCI combustion model and used it to control ignition delay and IMEP. They also conducted another study and developed a mode switching controller between Conventional Dual Fuel (CDF) operation and RCCI operation. (Indrajuana et al., 2018). Researchers also used the developed RCCI control-oriented models to study RCCI operation. Kakoee et al. (Kakoee et al., 2020) estimated combustion timing and load of an RCCI engine using their validated physics-based control-oriented model and proved the accuracy of estimations.

Experimental RCCI combustion controller designs initially used the PI controller strategy. Arora et al. (Arora and Shahbakhti, 2017) implemented a real-time closed-loop single input single output combustion controller to control CA50 during transient operation. Later Kondipati et al. (Kondipati et al., 2017) advanced Arora et al. work and implemented three PI controllers to track IMEP as well as CA50. Their designed controller selected dual fuel premixed ration (PR) or start of injection (SOI) of the in-cylinder injected fuel as the control action based on a sensitivity map and was able to reach desired control targets within 2-4 engine cycles. Model-based RCCI combustion controller design approach was used by a couple of researchers on a real RCCI engine. The first model-based RCCI MPC controller was accomplished by Raut et al. (Raut et al., 2018a), (Raut et al., 2018b). Their MPC controller was designed to track desired CA50 and IMEP by using SOI and fuel quanity (FQ) as control actions. The MPC controller tracked CA50 and IMEP with 1 CAD and 19.6 kPa average tracking errors, respectively.

Data-driven modeling (DDM) is a more recent approach in RCCI combustion controller design. This approach can reduce model development efforts significantly while reaching similar estimation accuracy compared to the physics-based modeling approach. Khoshbakht Irdmousa et al. (Irdmousa et al., 2019) developed and implemented the first validated data-driven RCCI dynamics model. The developed state-space model was used to design an MPC controller to control CA50 on a real RCCI engine. Basina

[1] United States National Science Foundation financially supported this research (Grants #1762520 and #1762595). The authors extend their appreciation to William Hansley from Michigan Technological University for his efforts on engine setup preparation.

10.1016/j.ifacol.2021.11.207

(Basina et al., 2020) also developed the first data-driven model to estimate maximum pressure rise rate (MPRR) for RCCI engines. These researches used known-states data-driven approach where the knowledge for selecting RCCI states is required and structure of the RCCI model needs to be known. Due to the complexity of RCCI combustion, the optimal selection of relevant states to represent RCCI combustion dynamics is challenging. This issue is addressed in the current research and a novel KCCA approach is implemented to develop a data-driven RCCI dynamic model based on unknown plant states. To the best knowledge of authors, this study presents: (i) the first RCCI combustion identification based on input-output approach with unknown model structure. (ii) the first constrained MPC controller design and implementation for an RCCI combustion.

This paper has following structure. The theory of KCCA based Linear Parameter Varying modeling is explained in Section 2, and the KCCA-LPV aplication into an RCCI engine is provided in Section 3. Section 4 discusses the physics-based RCCI dynamic model. Finally, the model predictive controller design and results for input-output-based MPC combustion controller for RCCI combustion is presented in Section 5.

2. KERNELIZED CANONICAL CORRELATION ANALYSIS BASED LINEAR PARAMETER VARYING MODELING

This study utilizes the state estimation approach developed by Rizvi et. al (Rizvi et al., 2018) to form an input-output based KCCA-LPV combustion model for an actual RCCI engine. A state-space dynamic model for an LPV system can be presented as shown in Eq. (1).

$$X_{k+1} = A(p_k)X_k + B(p_k)U_k + K(p_k)E_k, \quad (1a)$$
$$Y_k = C(p_k)X_k + E_k, \quad (1b)$$

where, U_k, Y_k, represent the inputs, the outputs, respectively. X_k denotes unknown states at discrete-time instant k. Matrices $A(p_k)$, $B(p_k)$, $K(p_k)$ and $C(p_k)$ denote LPV state-space matrices dependent on scheduling variables p_k. E_k notes additive Gaussian white noise. Eq. (1) can be updated by $E_k = Y_k - C(p_k)X_k$ to form state space model presented by Eq. (2).

$$X_{k+1} = \widetilde{A}(p_k)X_k + \widetilde{B}(p_k)U_k + K(p_k)E_k, \quad (2a)$$
$$Y_k = C(p_k)X_k + E_k, \quad (2b)$$

where $\widetilde{A}(p_k)$ and $\widetilde{B}(p_k)$ are represented by $B(p_k) - K(p_k)D(p_k)$ and $A(p_k) - K(p_k)C(p_k)$, respectively. Identification of $\widetilde{A}(p_k)$, $\widetilde{B}(p_k)$, $K(p_k)$ and $C(p_k)$ requires estimation of states (X_k) associated with measured U_k, Y_k data. LPV-SS formulation at Eq. (2) can be used to obtain future outputs as presented in Eq. (3).

$$\begin{bmatrix} Y_k \\ Y_{k+1} \\ \vdots \\ Y_{k+d+1} \end{bmatrix} = (\mathcal{O}_f^d \diamond p)_k X_k + (\mathcal{H}_f^d \diamond p)_k \begin{bmatrix} U_k \\ U_{k+1} \\ \vdots \\ U_{k+d+1} \end{bmatrix} + (\mathcal{L}_f^d \diamond p)_k \begin{bmatrix} Y_k \\ Y_{k+1} \\ \vdots \\ Y_{k+d+1} \end{bmatrix} + \begin{bmatrix} e_k \\ e_{k+1} \\ \vdots \\ e_{k+d+1} \end{bmatrix} \quad (3)$$

$(\mathcal{O}_f^d \diamond p)_k$ is the observability matrix at time k along with the scheduling trajectory p. $(\mathcal{H}_f^d \diamond p)_k$ is a forward Toeplitz matrix, and $((\mathcal{L}_f^d \diamond p)_k$ is a lower triangle matrix. Future measured outputs, implemented inputs, white noise, and scheduling parameter vectors for time instant k are collected to form matrices presented in Eq. (4a) till Eq. (4d).

$$\bar{Y}_{k+d}^d := [Y_k^\top \ \ldots \ Y_{k+d-1}^\top]^\top \quad (4a)$$
$$\bar{U}_{k+d}^d := [U_k^\top \ \ldots \ U_{k+d-1}^\top]^\top \quad (4b)$$
$$\bar{E}_{k+d}^d := [e_k^\top \ \ldots \ e_{k+d-1}^\top]^\top \quad (4c)$$
$$\bar{P}_{k+d}^d := [p_k^\top \ \ldots \ p_{k+d-1}^\top]^\top \quad (4d)$$

where d represents future data window size. Eq. (3) can be updated to by implementing definitions at Eq. (4) to form Eq. (5)

$$\bar{Y}_{k+d}^d = (\mathcal{O}_f^d \diamond p)_k X_k + (\mathcal{H}_f^d \diamond p)_k \bar{U}_{k+d}^d + (\mathcal{L}_f^d \diamond p)_k \bar{Y}_{k+d}^d + \bar{E}_{k+d}^d \quad (5)$$

Unknown states at time step k based on future inputs and outputs are computed from Eq. (5) and presented in Eq. (6).

$$X_k = (\mathcal{O}_f^d \diamond p)_k^{\dagger} \left((I - (\mathcal{L}_f^d \diamond p)_k)\bar{Y}_{k+d}^d - (\mathcal{H}_f^d \diamond p)_k \bar{U}_{k+d}^d \right) - (\mathcal{O}_f^d \diamond p)^{\dagger} \bar{E}_{k+d}^d \quad (6)$$

Since E is an independent zero-mean process noise which is identically distributed at experimental data, $(\mathcal{O}_f^d \diamond p)^{\dagger} \bar{E}_{k+d}^d$ is expected to be zero and can be eliminated. State estimation represented at Eq. (6) is simplified to Eq. (7) by defining $\bar{Z}_{k+d}^d = \begin{bmatrix} \bar{U}_{k+d}^d \\ \bar{Y}_{k+d}^d \end{bmatrix}$ as the collection of future plant inputs and outputs .

$$X_k = (\mathcal{O}_f^d \diamond p)_k^{\dagger} \left[-(\mathcal{H}_f^d \diamond p)_k \ I - (\mathcal{L}_f^d \diamond p)_k \right] \bar{Z}_{k+d}^d \quad (7)$$

Future mapping matrix can be defined as Eq. (8)

$$\varphi_f(\bar{p}_{k+d}^d) = (\mathcal{O}_f^d \diamond p)_k^{\dagger} \left[-(\mathcal{H}_f^d \diamond p)_k \ I - (\mathcal{L}_f^d \diamond p)_k \right] \quad (8)$$

and state estimation at time step k can be simply expressed as:

$$X_k = \varphi_f(\bar{p}_{k+d}^d) \bar{Z}_{k+d}^d \quad (9)$$

This approach is also applicable to past measurements to estimate unknown states at time step k based on stepwise output calculation from past d step measurement.

$$X_k = (\mathcal{X}_p^d \diamond p)_k X_{k-d} + (\mathcal{R}_p^d \diamond p)_k [U_{k-d} \ U_{k-d+1} \ \ldots \ U_{k-1}]^T + (\mathcal{V}_p^d \diamond p)_k [Y_{k-d} \ Y_{k-d+1} \ \ldots \ Y_{k-1}]^T \quad (10)$$

Past measured outputs, inputs, white noise, and scheduling parameter vectors for time instant k are denoted by $\bar{Y}_k^d$, $\bar{U}_k^d$, $\bar{E}_k^d$, and $\bar{P}_k^d$ and formed similar to future matrices at Eq. (4). These past measurements can be used to rewrite state estimation at Eq. (10).

$$X_k = (\mathcal{X}_p^d \diamond p)_k X_{k-d} + (\mathcal{R}_p^d \diamond p)_k \bar{U}_k^d + (\mathcal{V}_p^d \diamond p)_k \bar{Y}_k^d \quad (11)$$

Choosing d such that $(\mathcal{X}_p^d \diamond p)_k \approx 0$ and defining $\bar{Z}_k^d = \begin{bmatrix} \bar{U}_k^d \\ \bar{Y}_k^d \end{bmatrix}$, state estimation at Eq. (11) is expressed as Eq. (12).

$$X_k = \left[(\mathcal{R}_f^d \diamond p)_k \ (\mathcal{V}_f^d \diamond p)_k \right] \bar{Z}_k^d \quad (12)$$

State estimation at time step k based on the past data is simplified to Eq. (14) by defining $\varphi_p(\bar{P}_k^d)$ as the past mapping matrix.

$$\varphi_p(\bar{P}_k^d) = \left[(\mathcal{R}_f^d \diamond p)_k \ (\mathcal{V}_f^d \diamond p)_k\right] \tag{13}$$

$$X_k = \varphi_p(\bar{P}_k^d)\bar{Z}_k^d \tag{14}$$

The past data-based state estimation approach which is presented in Eq. (9) can be employed to obtain a collection of all estimated states at all time steps. This collection is named as Φ_p and defined in Eq. (15)

$$\Phi_p := \left[\varphi_p(\bar{P}_1^d)\bar{Z}_1^d \ \varphi_p(\bar{P}_2^d)\bar{Z}_2^d \ \ldots \ \varphi_p(\bar{P}_N^d)\bar{Z}_N^d\right]^\top \tag{15}$$

Φ_f is also defined as the collection of estimated states at all time steps based on the future data estimation method presented at Eq. (16).

$$\Phi_f = \left[\varphi_p(\bar{P}_{1+d}^d)\bar{Z}_{1+d}^d \ \varphi_p(\bar{P}_{2+d}^d)\bar{Z}_{2+d}^d \ \ldots \ \varphi_p(\bar{P}_{N+d}^d)\bar{Z}_{N+d}^d\right]^\top \tag{16}$$

Maximizing correlation between future data-based estimated states and past data-based estimated states can be accomplished by Canonical Correlation Analysis (CCA) method. The CCA problem with respected past data based estimated states and future data based estimated states is provided by the following description:

$$\underset{v_j, w_j}{max} \ v_j^\top \Phi_f^\top \Phi_p w_j \quad s.t. \quad v_j^\top \Phi_f^\top \Phi_f v_j = w_j^\top \Phi_p^\top \Phi_p w_j = 1 \tag{17}$$

Solution for the regularized CCA formation can be obtained by Lagrangian formation represented by Eq. (18).

$$\mathcal{L}(v_j, w_j, s, r) = \mathcal{J}(v_j, w_j, s, r) - \sum_{k=1}^{N} \eta_j^k (s_k - v_j^\top \varphi_f(\bar{P}_{k+d}^d)\bar{Z}_{k+d}^d) - \sum_{k=1}^{N} \kappa_j^k (s_k - v_j^\top \varphi_f(\bar{P}_k^d)\bar{Z}_k^d) \tag{18}$$

where $\eta_j = [\eta_j^1 \ \ldots \ \eta_j^N]^\top$ and $\kappa_j = [\kappa_j^1 \ \ldots \ \kappa_j^N]^\top$ are Lagrangian multipliers. The global minimum is computed where derivatives with respect to Lagrangian function variables are zero. Lagrange problem can be converted to the following generalized eigenvalue problem.

$$K_p p \kappa_j = \lambda_j (v_f K_f f + I)\eta_j \tag{19a}$$

$$K_f f \eta = \lambda_j (v_f K_f f + I)\kappa_j, \tag{19b}$$

where $K_{pp} = \Phi_p \Phi_p^\top$ and $K_{ff} = \Phi_f \Phi_f^\top$. Lagrangian multipliers are the solution of the generalized eigen value problem presented in Eq. (19). Finally, Lagrangian multipliers are used to compute the estimated states as

$$X_k^j = \kappa_j \begin{bmatrix} (\bar{Z}_1^d)^T \bar{k}(\bar{P}_1^d, \bar{P}_k^d) \\ (\bar{Z}_2^d)^T \bar{k}(\bar{P}_2^d, \bar{P}_k^d) \\ \vdots \\ (\bar{Z}_N^d)^T \bar{k}(\bar{P}_N^d, \bar{P}_k^d) \end{bmatrix} = \eta_j \begin{bmatrix} (\bar{Z}_{1+d}^d)^T \bar{k}(\bar{P}_{1+d}^d, \bar{P}_{k+d}^d) \\ (\bar{Z}_{2+d}^d)^T \bar{k}(\bar{P}_{2+d}^d, \bar{P}_{k+d}^d) \\ \vdots \\ (\bar{Z}_{N+d}^d)^T \bar{k}(\bar{P}_{N+d}^d, \bar{P}_{k+d}^d) \end{bmatrix} \tag{20}$$

Estimated states through the KCCA method can be used along with measured inputs and outputs to obtain a state-space dynamic model of the RCCI engine. This research utilizes the least-squared SVM (LS-SVM) method which is explained at (Irdmousa et al., 2019) to determine the dynamic state space matrices $\tilde{A}(p_k), B(p_k), C(p_k)$, and $K(p_k)$ at Eq. (2).

3. KCCA-LPV MODELING OF AN RCCI ENGINE

The presented method from section 2 is used to develop a control-oriented combustion model for an RCCI engine. Experimental data were obtained from a 2-liter 4-cylinder RCCI engine. Fig. 1 presents the RCCI engine, AC dynamometer, fuel supply system and data acquisition setup. Inputs to the plant and measurable outputs from the plant are defined in Eq. (21) and (22), respectively.

$$U = [PR \ SOI \ FQ]^T, \tag{21}$$

$$Y = [CA50 \ IMEP]^T. \tag{22}$$

Input n-heptane SOI, PR, and FQ were varied and CA50, IMEP were computed from acquired pressure traces. Scheduling variable was considered to be fuel quantity as it is the primary parameter to affect engine load (IMEP) and affects the RCCI engine dynamics. Fig. 2 presents a sample of acquired experimental data at PR=10 and varied FQ and SOI values. The collected experimental data were split into training data and test data sets. Training data set which includes 65% of the data is used by KCCA-LPV

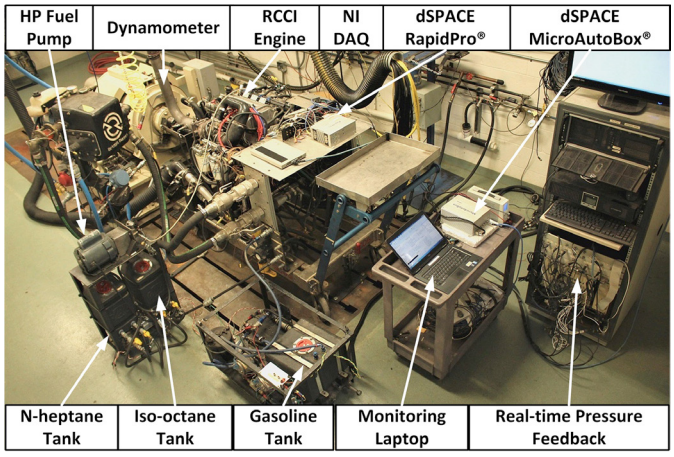

Fig. 1. The experimental RCCI engine setup.

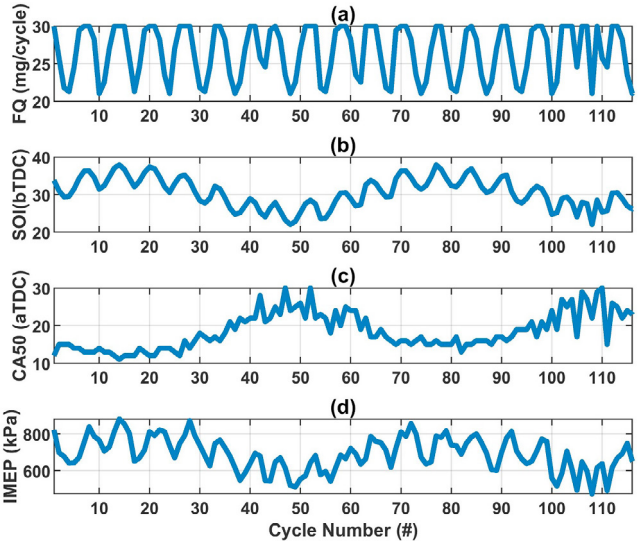

Fig. 2. Training data from the RCCI engine at $T_{in} = 333$ K, $N = 1200$ RPM, $P_{in} = 96.5$ kPa, $PR = 10$.

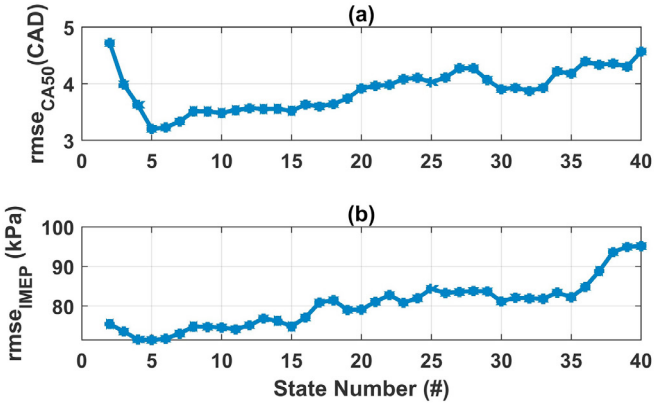

Fig. 3. The effect of unknown states number on model identification accuracy.

approach to estimate unknown states. This leads finding Lagrangian multipliers α and β for the representation of the RCCI combustion dynamics. Computed Lagrangian multipliers are used to estimate state space at Eq. (1). The developed LPV representation is then used to estimate the plant output at the remaining 35% of the data which was reserved as the test data.

$$\begin{bmatrix} X_1 \\ X_2 \\ X_3 \\ X_4 \\ X_5 \end{bmatrix}_{k+1} = A(FQ) \begin{bmatrix} X_1 \\ X_2 \\ X_3 \\ X_4 \\ X_5 \end{bmatrix}_{k} + B(FQ) \begin{bmatrix} SOI \\ FQ \\ PR \end{bmatrix}_{k}, \tag{23a}$$

$$\begin{bmatrix} CA50 \\ IMEP \end{bmatrix}_{k+1} = C(FQ) \left[X_1 X_2 X_3 X_4 X_5 \right]^T_{k+1}, \tag{23b}$$

The KCCA-LPV modeling approach allows states to be

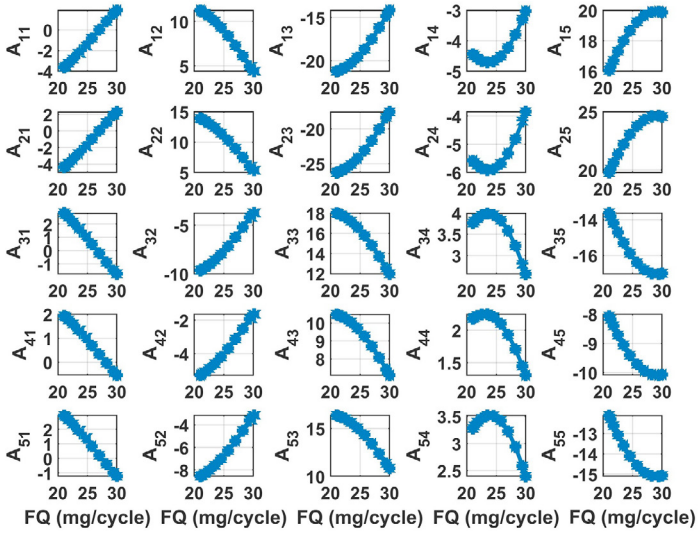

Fig. 4. LPV representaion of "A" matrix by KCCA identification, representing RCCI dynamics in a state-space model.

independent of outputs and consequently states numbers can be varied to obtain the best estimation accuracy for the test data. Fig. 3 presents the effect of estimated state size on estimation accuracy for CA50 and IMEP. The KCCA-LPV model accuracy reaches the highest accuracy when KCCA uses five unknown states at each time step.

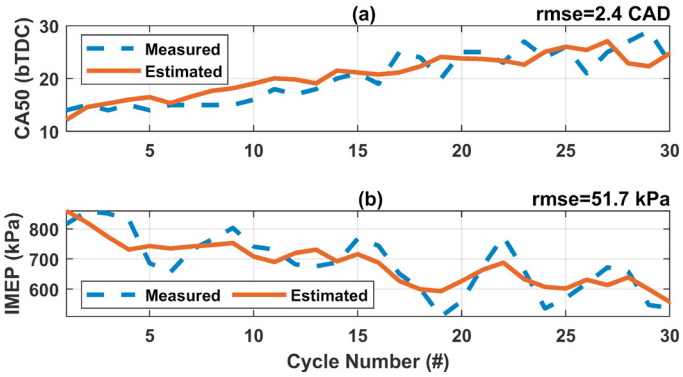

Fig. 5. Performance of the identified input-output LPV model at $T_{in} = 333$ K, $N = 1200$ RPM, $P_{in} = 96.5$ kPa, $PR = 14$.

Therefore, state numbers are selected to be five, and state-space representation of the RCCI combustion is represented as Eq. (23). Fig. 4 shows dependency of identified A matrix elements on fuel quantity as the scheduling variable. It can be observed that these elements vary significantly with the scheduling variable variation as we expect from a typical LPV system. Fig. 5 verifies performance of the KCCA-LPV model to estimate CA50 and IMEP with 2.4 CAD and 51.7 kPa estimation error, respectively. The developed LPV model is later used to control CA50 and IMEP on a experimentally validated physics-based RCCI model. (Basina et al., 2020).

4. DATA-DRIVEN MODEL-BASED PREDICTIVE COMBUSTION CONTROLLER DESIGN

This study utilizes the MPC strategy because of its capacity to handle states and actuators' constraints and to predict future plant outputs and consider them during MPC optimization process. Here, a constrained MPC platform (Fig. 6) is developed to follow the referenced CA50 and IMEP through five engine cycles as the prediction horizon while computing optimum n-heptane SOI, injected fuel quantity, and PR as the control variables. The designed MPC controller uses the KCCA-LPV RCCI combustion model to obtain system dynamics. The data-driven

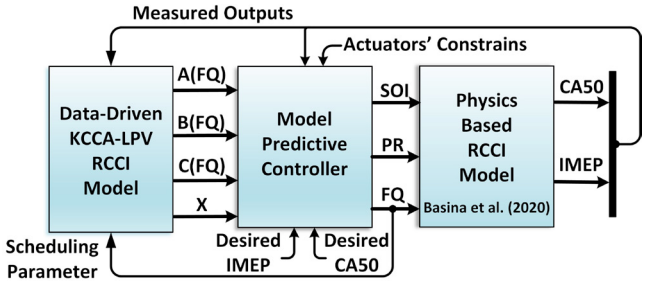

Fig. 6. Schematic of the designed data-driven input-output identified MIMO model predictive controller.

KCCA-LPV model adjusts the RCCI dynamics based on changing fuel quantity as the scheduling parameter. It also receives measured plant outputs and computes the unknown plant states. The computed state-space matrices and unknown states are provided to the MPC controller to compute optimized control actions based on desired

outputs, measured outputs, and actuators' constraints. The decided control actions are then implemented on the validated physics-based RCCI model to test the controller efficiency of the KCCA based constrained MIMO MPC controller. The discrete time state-space dynamic model of an RCCI combustion which is presented at Eq. (23), can be used to iteratively compute plant output through the prediction horizon. Eq. (24) represents the predicted plant output through prediction horizon based on plant information at beginning of the horizon.

$$\mathbb{Y}_k = \Omega X(k_i) + \Phi \mathbb{U}_k, \tag{24}$$

$\mathbb{Y}_k$ and $\mathbb{U}_k$ are vectors denoting plant outputs and plant inputs at prediction horizon.

$$\begin{aligned}\mathbb{Y}_k = [Y(k_i+1|k_i) \;\; Y(k_i+2|k_i) \;\; Y(k_i+3|k_i) \\ Y(k_i+4|k_i) \;\; Y(k_i+5|k_i)]^\top,\end{aligned} \tag{25}$$

$$\mathbb{U}_k = [U(k_i) \;\; U(k_i+1) \;\; U(k_i+3)U(k_i+3) \;\; U(k_i+4)]^\top, \tag{26}$$

$Y(k_i+N|k_i)$ represents the forecasted plant output at step k_i+N using plant knowledge at step k_i; $U(k_i+N)$ represents control action at step k_i+N. Prediction matrices Ω and Φ are computed based on state-space $A(FQ)$, $B(FQ)$, and $C(FQ)$ matrices from Eq. (23).

$$\Omega = \begin{bmatrix} CA \\ CA^2 \\ CA^3 \\ CA^4 \\ CA^5 \end{bmatrix}; \Phi = \begin{bmatrix} CB & 0 & 0 & 0 & 0 \\ CAB & CB & 0 & 0 & 0 \\ CA^2B & CAB & CB & 0 & 0 \\ CA^3B & CA^2B & CAB & CB & 0 \\ CA^4B & CA^3B & CA^2B & CAB & CB \end{bmatrix} \tag{27}$$

MPC optimization strategy considers to minimize prediction tracking error with minimized control action efforts. This strategy is formulated by the cost function presented at Eq. (28).

$$J = \sum_{i=1}^{N} [(\Psi_i - Y_i)^\top Q(\Psi_i - Y_i) + U_i^\top R U_i], \tag{28}$$

where desired outputs through the prediction horizon are denoted by Ψ. The weighting matrices through the prediction horizon on tracking errors and magnitude of control variables are shown by Q and R, respectively. Eq. (28) is used to generate MPC cost function at Eq. (29).

$$\begin{aligned}J = (\Psi - \Omega x(k_i))^\top (\Psi - \Omega x(k_i)) \\ -2\Delta\mathbb{U}^\top \Phi^\top (\Psi - \Omega x(k_i)) + \Delta\mathbb{U}^\top (\Phi^\top \Phi + R)\Delta\mathbb{U},\end{aligned} \tag{29}$$

Constraints on the rate and magnitude of control action can be represented by Eq. (30).

$$M\Delta\mathbb{U} \leq \gamma, \tag{30}$$

where M, $\Delta\mathbb{U}$ and γ are defined as

$$\Delta\mathbb{U} = \begin{bmatrix} \Delta U(k_i) \\ \Delta U(k_i+1) \\ \Delta U(k_i+2) \\ \Delta U(k_i+3) \\ \Delta U(k_i+4) \end{bmatrix}; \Delta U = \begin{bmatrix} \Delta FQ \\ \Delta SOI \\ \Delta PR \end{bmatrix} \tag{31}$$

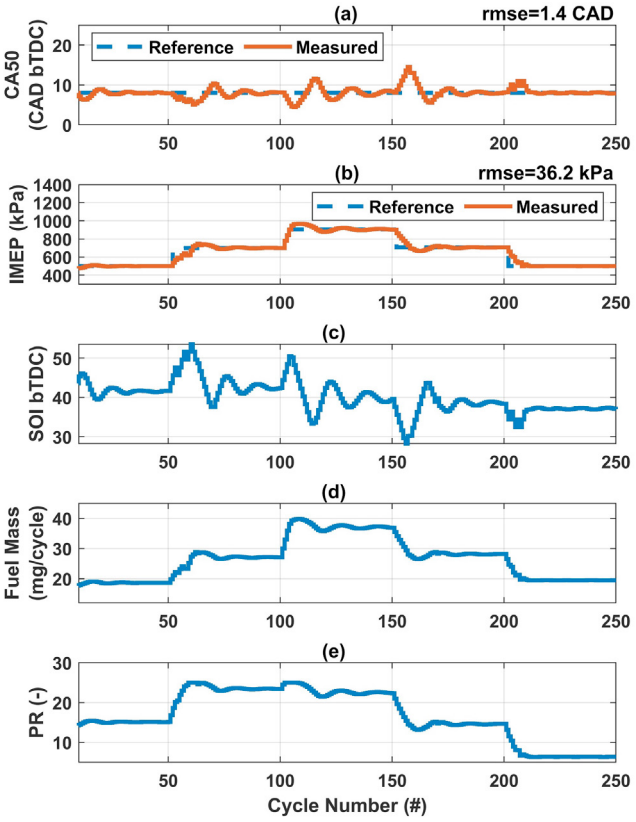

Fig. 7. Constrained MIMO MPC results (a) maintaining desired CA50 tracking, (b) load trajectory tracking, control actions: (c) start of injection timing, (d) fuel quantity , (e) premixed ratio.

$$M = \begin{bmatrix} I_3 & 0_{3,3} & 0_{3,3} & 0_{3,3} & 0_{3,3} \\ 0_{3,3} & I_3 & 0_{3,3} & 0_{3,3} & 0_{3,3} \\ 0_{3,3} & 0_{3,3} & I_3 & 0_{3,3} & 0_{3,3} \\ 0_{3,3} & 0_{3,3} & 0_{3,3} & I_3 & 0_{3,3} \\ 0_{3,3} & 0_{3,3} & 0_{3,3} & 0_{3,3} & I_3 \\ -I_3 & 0_{3,3} & 0_{3,3} & 0_{3,3} & 0_{3,3} \\ 0_{3,3} & -I_3 & 0_{3,3} & 0_{3,3} & 0_{3,3} \\ 0_{3,3} & 0_{3,3} & -I_3 & 0_{3,3} & 0_{3,3} \\ 0_{3,3} & 0_{3,3} & 0_{3,3} & -I_3 & 0_{3,3} \\ 0_{3,3} & 0_{3,3} & 0_{3,3} & 0_{3,3} & -I_3 \\ I_3 & 0_{3,3} & 0_{3,3} & 0_{3,3} & 0_{3,3} \\ I_3 & I_3 & 0_{3,3} & 0_{3,3} & 0_{3,3} \\ I_3 & I_3 & I_3 & 0_{3,3} & 0_{3,3} \\ I_3 & I_3 & I_3 & I_3 & 0_{3,3} \\ I_3 & I_3 & I_3 & I_3 & I_3 \\ -I_3 & 0_{3,3} & 0_{3,3} & 0_{3,3} & 0_{3,3} \\ -I_3 & -I_3 & 0_{3,3} & 0_{3,3} & 0_{3,3} \\ -I_3 & -I_3 & -I_3 & 0_{3,3} & 0_{3,3} \\ -I_3 & -I_3 & -I_3 & -I_3 & 0_{3,3} \\ -I_3 & -I_3 & -I_3 & -I_3 & -I_3 \end{bmatrix}; \gamma = \begin{bmatrix} \Delta U_{max} \\ \Delta U_{max} \\ \Delta U_{max} \\ \Delta U_{max} \\ \Delta U_{max} \\ -\Delta U_{min} \\ -\Delta U_{min} \\ -\Delta U_{min} \\ -\Delta U_{min} \\ -\Delta U_{min} \\ U_{max} - U \\ U_{max} - U \\ U_{max} - U \\ U_{max} - U \\ U_{max} - U \\ U_{min} + U \\ U_{min} + U \\ U_{min} + U \\ U_{min} + U \\ U_{min} + U \\ U_{min} + U \end{bmatrix} \tag{32}$$

Lagrangian optimization process is used to minimize MPC cost function at Eq. (29) while considering constraints on rate and magnitude of control action represented at Eq. (30). Lagrangian optimization can be represented as

$$\underset{\lambda \geq 0}{max} \underset{\Delta\mathbb{U}}{min} [\frac{1}{2}\Delta\mathbb{U}^T E \Delta\mathbb{U} + \Delta\mathbb{U}^T F + \lambda^T (M\Delta\mathbb{U} - \gamma)] \tag{33}$$

E and F matrices are defined as:

$$E = 2(\Phi^\top \Phi + R) \tag{34}$$

$$F = 2(\Phi^\top \Phi + R)\Phi^\top (\Psi - \Omega x(k_i)) \tag{35}$$

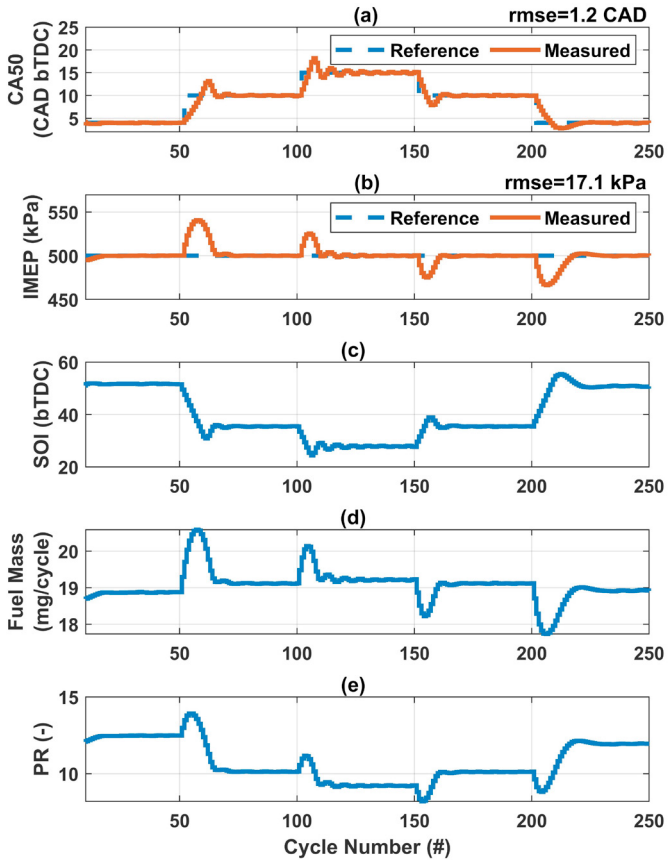

Fig. 8. Constrained MIMO MPC results (a) CA50 trajectory tracking, (b) Maintaining desired load tracking, control actions: (c) start of injection timing, (d) fuel quantity, (e) premixed ratio variations.

The optimal solution is derived to be

$$\Delta\mathbb{U} = -E^{-1}F - E^{-1}M^T\lambda^* \tag{36}$$

where λ^* is the solution for the Lagrangian multiplier. This research utilizes Hildret quadratic programming method to perform the following iterative method to compute λ^*

$$\lambda_i^{m+1} = max(0, w_i^{m+1}) \tag{37}$$

where w_i^{m+1} is computed as

$$w_i^{m+1} = -\frac{1}{l_{ii}}[k_i + \sum_{j=1}^{i-1} l_{ij}\lambda_j^{m+1} + \sum_{j=i+1}^{n} l_{ij}\lambda_j^m] \tag{38}$$

where l_{ij} is the ijth entry in the L matrix and k_i is the ith element in the K matrix. L and K matrices are defined as

$$L = ME^{-1}M^T; K = \gamma + ME^{-1}F \tag{39}$$

Fig. 7 presents the MPC controller performance to track step changes at IMEP and fixed CA50. The controller was able to track desired values with 1.4 CAD and 36.2 kPa errors respectively. A similar test was conducted for fixed desired IMEP and step changes at desired CA50. Fig. 8 shows tracking performance and computed control actions. The controller followed the desired IMEP and CA50 with 1.2 CAD and 17.1 kPa tracking errors, respectively.

5. CONCLUSIONS

This paper introduced the first Kernelized Canonical Correlation Analysis based LPV state-space dynamic model for an RCCI engine combustion and the first constrained MPC controller for RCCI combustion. Experimental measurements were obtained from an RCCI engine by changing start of injection timing, premixed ratio and fuel quantity as the control inputs and measuring CA50 and IMEP as the outputs. These data were then used to estimate unknown states and create a data-driven LPV model to determine CA50 and IMEP as a function of three control inputs. The LPV model was later connected into a constrained MPC framework to track reference CA50 and IMEP. The developed controller results showed that the KCCA-LPV based constrained MPC controller followed the referenced CA50 and IMEP with less than 1.4 CAD and 37 kPa average tracking errors, respectively.

REFERENCES

Arora, J.K. and Shahbakhti, M. (2017). Real-time closed-loop control of a light-duty RCCI engine during transient operations. Paper No. 2017-01-0767.

Basina, L.A., Irdmousa, B.K., Velni, J.M., Borhan, H., Naber, J.D., and Shahbakhti, M. (2020). Data-driven modeling and predictive control of maximum pressure rise rate in RCCI engines. In *Control Technology and Applications (CCTA)*, Pages: 94–99. IEEE.

Indrajuana, A., Bekdemir, C., Feru, E., and Willems, F. (2018). Towards model-based control of RCCI-CDF mode-switching in dual fuel engines. Technical report, SAE Technical Paper. Paper No. 2018-01-0263.

Indrajuana, A., Bekdemir, C., Luo, X., and Willems, F. (2016). Robust multivariable feedback control of natural gas-diesel RCCI combustion. *IFAC-PapersOnLine*, 49(11), Pages: 217–222.

Irdmousa, B.K., Rizvi, S.Z., Veini, J.M., Naber, J., and Shahbakhti, M. (2019). Data-driven modeling and predictive control of combustion phasing for RCCI engines. In *2019 American Control Conference (ACC)*, Pages: 1617–1622. IEEE.

Kakoee, A., Bakhshan, Y., Barbier, A., Bares, P., and Guardiola, C. (2020). Modeling combustion timing in an RCCI engine by means of a control oriented model. *Control Engineering Practice*, 97, Pages: 104321.

Khodadadi Sadabadi, K., Shahbakhti, M., Bharath, A.N., and Reitz, R.D. (2016). Modeling of combustion phasing of a reactivity-controlled compression ignition engine for control applications. *International Journal of Engine Research*, 17(4), Pages: 421–435.

Kondipati, N.N.T., Arora, J.K., Bidarvatan, M., and Shahbakhti, M. (2017). Modeling, design and implementation of a closed-loop combustion controller for an RCCI engine. In *2017 American Control Conference (ACC)*, Pages: 4747–4752. IEEE.

Raut, A., Irdmousa, B.K., and Shahbakhti, M. (2018a). Dynamic modeling and model predictive control of an RCCI engine. *Control Engineering Practice*, 81, Pages: 129–144.

Raut, A., Bidarvatan, M., Borhan, H., and Shahbakhti, M. (2018b). Model predictive control of an RCCI engine. In *2018 American Control Conference (ACC)*, Pages: 1604–1609. IEEE.

Rizvi, S.Z., Velni, J.M., Abbasi, F., Tóth, R., and Meskin, N. (2018). State-space LPV model identification using kernelized machine learning. *Automatica*, 88, Pages: 38–47.